Proceedings of ERAD (2004): 261–267 © Copernicus GmbH 2004

ERAD 2004

How do updrafts and embedded convection influence riming?

B. Baschek, R. Schefold, and E. Barthazy

Institute for Atmospheric and climate science, ETH, Zürich, Switzerland

Abstract. Experimental observations of the riming degree of ice crystals together with a quantification of embedded convective cells resp. of difficult to measure updrafts are scarce. Though their interrelation is generally acknowledged, a more detailed understanding of these processes is of interest for, e.g. high resolution weather modelling and the interpretation of radar data.

During the field campaign RAMS I (Riming, Aggregation and Mass of Snowflakes) precipitating clouds have been observed by the mobile high-resolution, vertically pointing X-band radar (ETH Zürich) from the base of a mountain. Properties of the same cloud are measured in-situ at the top of the mountain by the HVSD (Hydrometeor Velocity and Shape detector). Additionally the degree of riming is determined by Formvar samples. The radar Doppler velocity is a combination of vertical wind speed and particle fall velocity. The HVSD measures the latter directly. A method has been developed to correct for the time lag between the measurements at the two stations through cross-correlation. By combining remote sensing and in-situ measurements, vertical winds can be estimated.

For several case studies, correlations between the degree of riming and vertical winds resp. a convective index - based only on radar data – have been found. The correlation coefficients are approximately -0.6 with a variation for different cases resp. parameters or filtering methods. The degree of riming increased with increasing strength of updrafts.

1 Introduction

This work is considering two different kinds of phenomena – a microphysical one (riming) and a dynamical one (embedded convection) – and their coupling. Riming is the freezing of super-cooled cloud droplets on snow crystals. It is, besides deposition and aggregation, one of the fundamental snow growing mechanisms. The connection between updrafts, causing condensation, and riming is generally acknowledged. However, experimental observations of the riming degree of ice crystals together with a quantification of updrafts resp. embedded convective cells are scarce. How can vertical winds be measured? What are suitable means for a quantification of embedded convective cells? What are the relevant time scales, which differ embedded convection from updrafts and what orographic influences are there? What are the correlations to the microphysics of riming? The better understanding of these processes are of interest for, e.g. high resolution weather modelling and the interpretation of radar data.

Correspondence to: B. Baschek
(Bjoern.Baschek@env.ethz.ch)

2 Setup of measurements for RAMS I

To answer some of the open questions, the field experiment RAMS I (Riming, Aggregation and Mass of Snowflakes) has been taking place at Mount Rigi in the Swiss Alps. This mountain has a steep rising front pointing towards the lowlands and the main weather direction. The setup (Fig. 1) is split up in two locations – one at the base and one close to the top. The steepness of the mountain allows to measure variables on different height levels at similar horizontal position. A precipitating cloud is observed by the mobile vertically pointing X-band Doppler radar (ETH Zürich) with 1 s temporal and 50 m spatial resolution from the foot of the mountain. The radar is at 450 m above sea level, which is usually below the melting layer, and is measuring and saving the full Doppler spectrum of the precipitation particles with 0.125 m/s velocity resolution. For measuring the raindrop size distribution, a Joss-Waldvogel-disdrometer is used. Radio soundings are performed and the wind field around the experimental site is monitored with one resp. two C-band Doppler radars, working in single- resp. dual-Doppler mode (Wüest, 2001). Properties of particles from the same cloud are measured in-situ close to the top of the mountain (1600 m above sea level, 1150 m above the radar). The snowfall

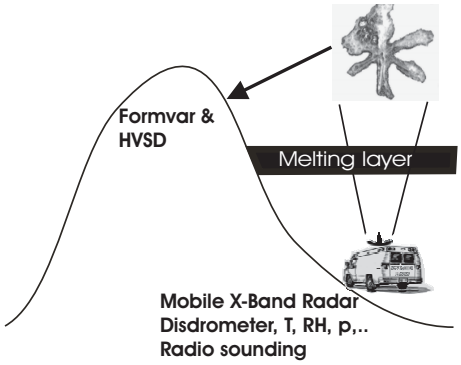

Fig. 1. Setup scheme with two locations, one at the base and the second close to the top of the mountain.

Table 1. Classification of riming with increasing number of accreted cloud droplets (Mosimann, 1995).

Riming Degree	Description
0	unrimed
1	lightly rimed
2	moderately rimed
3	densely rimed
4	heavily rimed
5	graupel

is observed with a hydrometeor velocity and shape detector (HVSD, see Barthazy et al. (2004 in press) or Schefold (2004) for more details), measuring shapes and the size distribution of the ice particles and their fall velocities, which are influenced by the degree of riming. In addition, ice crystals are replicated with the Formvar method (Schaefer, 1956) to determine their size, type and riming degree. This combination of remote sensing and in-situ measurements gives a multitude of information.

3 Degree of riming

Different methods and scales exist for the determination of the degree of riming – the amount of accreted super-cooled cloud water on ice crystals. In this study a scale of six classes (Table 1; examples Fig. 2), with increasing number of frozen on cloud droplets, has been used (Mosimann et al., 1994). The samples have been achieved with help of the Formvar replication method (Schaefer, 1956). Riming is not only an important growing mechanism, but it is also important for scavenging, the transfer of pollutants from the atmosphere into the snow (Poulida et al., 1998).

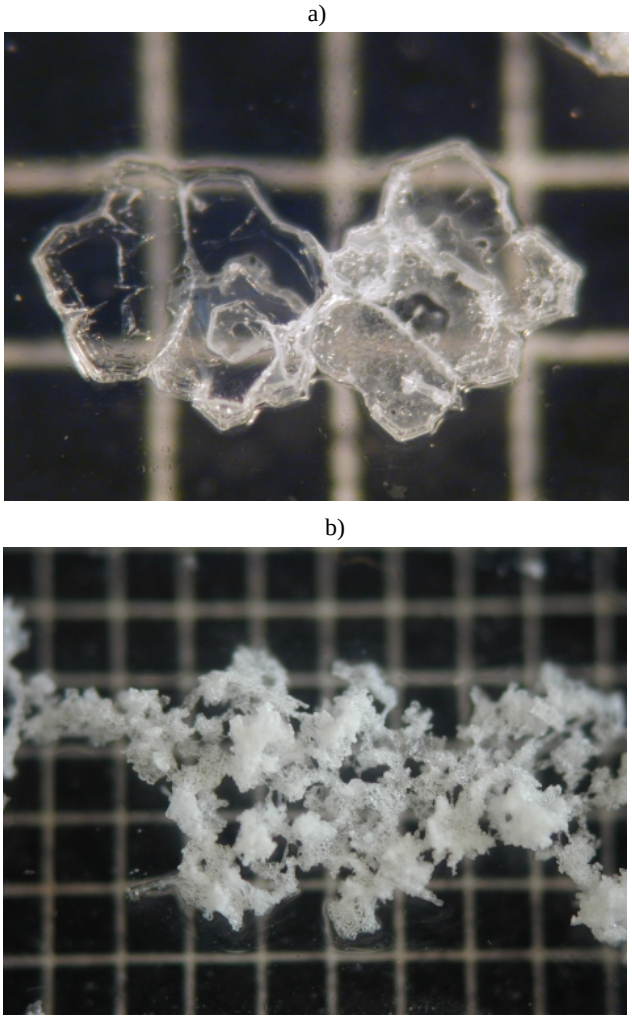

Fig. 2. Formvar replica of an unrimed (class 0) crystal (a) and of a densely rimed (class 3) snowflake (b) – grid size 1 mm.

4 Quantification of convection based on radar data only

Embedded convective cells or "cellular overturning" (Houze and Medina, 2003) in stratiform (Houze, 1997) precipitation could be a reason for riming. The classical separation into stratiform and convective regimes of precipitation is quite rough. A more detailed classification is needed for finding a connection between embedded convection and riming and for explaining differences in the degree of riming. Classification of convection has been made before; by, e.g. Mosimann (1995) for vertical X-band radars via the variability of the mean Doppler velocity with a convection index,

$$\kappa = \frac{|\,\mathrm{v} - <\mathrm{v}>_t\,|}{<\mathrm{v}>_t} \quad , \tag{1}$$

as introduced by Mosimann (1995), which bases on data of vertically pointing radars. The numerator term $|\mathrm{v}-<\mathrm{v}>_t|$ is a measure of the variability of the Doppler velocity, with v being the Doppler velocity at a certain time and height and

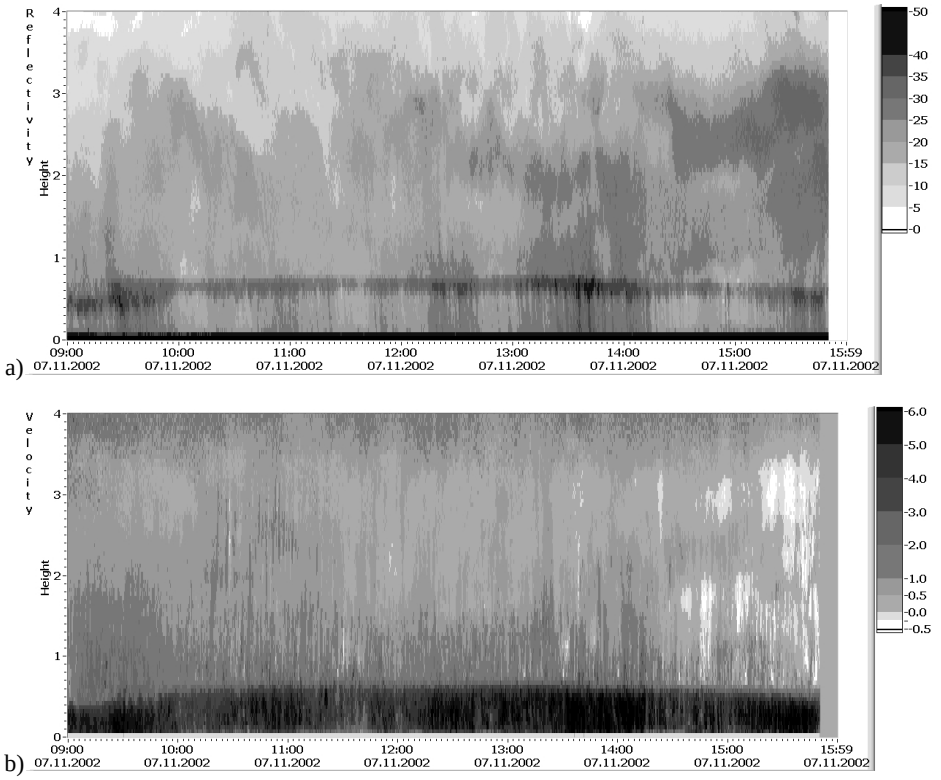

Fig. 3. Height time diagram (HTI) of reflectivity (a, [dBZ]) and Doppler velocity (b, [m/s]) for a 7 h period on 7 November 2002. An increasing number of embedded convective cells can be seen.

$< \mathrm{v} >_t$ the average over a period of time (in our study 5 minutes) at constant height. The average velocity as denominator term $< \mathrm{v} >_t$, gives smaller absolute changes of κ with fluctuations for higher average velocities. With the above definition the value of κ is becoming negative for negative average Doppler velocities.

The equation provides a value for every height step. If wanting to follow the growth history of a snow crystal and to consider how convective its environment has been during its formation, an integration or averaging of κ over height is a possibility. But for this the above definition of κ is not suitable. First because it has a singularity for an average velocity of 0 m/s. Second because negative values of κ, which are describing even more convective situations, could cancel with positive values while averaging. As a straight forward method a modified convection index κ_{mod} (Eq. 2) has been chosen:

$$\kappa_{mod} = \begin{cases} \alpha & \kappa \geq \alpha \text{ or } \kappa \leq 0, \\ \kappa & \text{else.} \end{cases} \quad (2)$$

The original κ is cut at a constant value α and the same value α is given to negative κ. For a comparison with riming, convectivity is computed by averaging κ_{mod} over height (Eq. 3; n = number of height steps) and multiplied by a second constant β; with $\alpha \cdot \beta = 5$.

$$\text{Convectivity} = \beta \cdot \Big(\sum_{\text{height}_0}^{\text{height}_1} \kappa_{\text{mod}}\Big)/\text{n} \quad (3)$$

This gives the same value range between 0 and 5, as the riming degree. For the following case studies $\alpha = 0.6$ and thus $\beta = 8.3$ have been chosen. Depending on the time scale for averaging, this convection index is strongly influenced by the vertical winds, but only one instrument is needed for its determination.

5 Estimation of vertical winds

The Doppler velocity, measured by a vertically pointing radar, is a combination of particle fall velocity and vertical wind speed. The combination of remote sensing and in-situ measurements gives the possibility to eliminate the influence of particle fall velocities, because the HVSD measures the particle fall velocities directly. After a lag time correction through cross-correlation of the data sets of radar and HVSD can thus the vertical winds be estimated (disdrometers could be used in a similar way in rain).

The radar is measuring the reflectivity and the Doppler spectrum in "free air". The Doppler velocity v_D is defined as the first moment of the velocity distribution,

$$\mathrm{v}_{D,\text{radar}} = \frac{\int_{-\infty}^{+\infty} \mathrm{z_v} \cdot \mathrm{v} \cdot \mathrm{dv}}{\mathrm{z}} . \quad (4)$$

For a vertically pointing radar, the velocity v (Eq. 5) is the sum of the "intrinsic" terminal fall velocity v_T of the particles and the vertical wind speed w (updrafts negative sign; v,

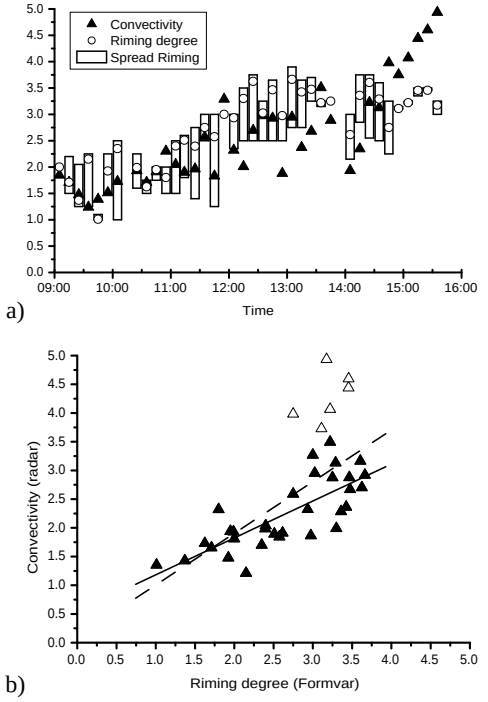

Fig. 4. Change in riming degree and convectivity versus time (a) and scatter plot of convectivity versus riming degree (b). The data points of the last one and a half hours are marked with the empty triangles. The straight lines are fits with (dashed) and without (solid) these last data points.

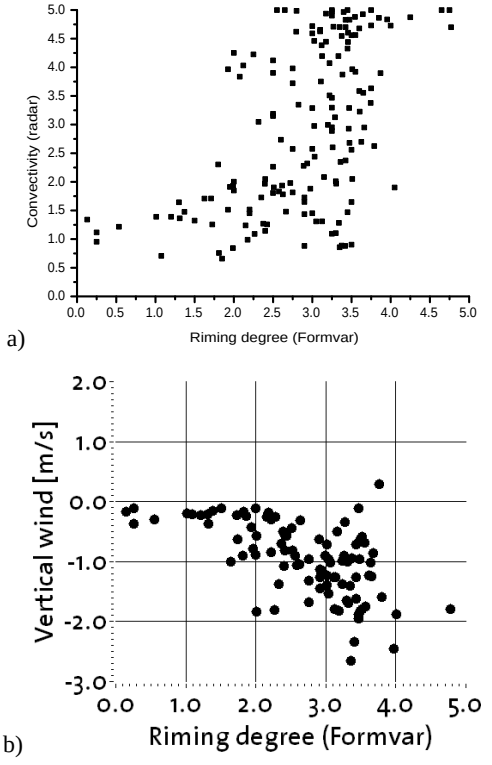

Fig. 5. Scatter plot of convectivity (a) with average time 5 min and vertical winds (b) averaged over eleven one minute values versus riming degree for 90 Formvar samples of all 9 cases of winter 02/03 of RAMS I.

v_T positive for falling particles), if assuming, that all particles are equally influenced by the vertical wind.

$$v_{radar} = v_T + w \tag{5}$$

The HVSD is measuring size distribution and velocity of hydrometeors at the ground. With the boundary condition, that vertical winds are zero ($w = 0$) at the ground, the measured velocity is for each particle equal to the intrinsic fall velocity: $v_{HVSD} = v_T$.

The particles measured by the HVSD can be split into velocity bins. If the radar reflectivity is computed separately for these bins, a Doppler spectrum is achieved. For solid ice one could compute the reflectivity via the "reflectivity factor" $\sum D^6$, with consideration of the smaller dielectric factor for ice spheres. For other types of ice particles, one has to correct for the lower densities. In this study, a mass-size-relation for graupel-like snow of medium density has been chosen (Locatelli and Hobbs, 1974) to compute the reflectivity - assuming Rayleigh scattering. For the computation of the Doppler velocity via the first moment only the shape of the spectrum is relevant, the scaling has no influence. Thus, only errors in the exponent of the assumed mass-size-relation play a role. Furthermore, by comparison of the zeroth moment of the Doppler spectrum received from the HVSD with the reflectivity measured by the radar, a test of the assumptions during the calculation can be performed. Problematic situations with strong vertical wind shear might be recognizable by comparing the computed with the measured Doppler spectra.

Finally, the vertical wind speed above the radar at the height level of the HVSD can be estimated. Therefore, the Doppler velocity, computed via the first moment of the HVSD Doppler spectrum, has to be subtracted from the Doppler velocity, measured by the radar at the equivalent height of the mountain station:

$$w = v_{D,radar} - v_{D,\mathrm{HVSD}} \tag{6}$$

Thus, a separation of the influence of steady vertical winds from the influence of embedded convection on riming can be done for this height level.

6 Case study

A convective index (see Sect. 4) – based on the X-band radar data - is used to quantify embedded convection in stratiform precipitation. For several case studies, a coupling between the degree of riming and this index resp. vertical winds (estimated by the method described in Sect. 5) is shown. From the case studies, which have been taking place in the winter season 2002/2003, as an example 7 November 2002 has

been chosen. Precipitation was caused by an occlusion. In the chosen 7 hour period, the rain rates were relatively low (per minute rain rate up to 7.3 mm/h, with 0.7 mm/h average and 4.7 mm in total). Temperature at the lower station rose from 4.1° to 6.2°C, falling again for the last half hour. At the top station, the temperature ranged between −1.5° and −2°C. Figure 3 shows the height-time-indicator (HTI) of reflectivity (a) and of the Doppler velocity (b) for this period. A bright band with varying strength and an increasing number and size of areas with close to zero or negative Doppler velocities – a clear indication of embedded convective cells – can be seen. The increase in cellular structure can even be seen in the reflectivity HTI.

The modified convection index has been computed, applying Eq. (3), and averaged over the height range 2 km above the height level of the top station. The result is shown in Fig, 4a together with riming. The degree of riming is estimated from analysis of the Formvar samples, taken at the top station. At the beginning of the period, the degree of riming has been about 1.5, started then to rise and had at the end of the period a degree of about 3.5. For computing the correlation between riming degree and convectivity, the convectivity has been averaged over the 10 min periods around the Formvar sampling times (38 in total). A scatter diagram of convectivity versus riming degree is shown in Fig. 4b. The computed correlation is 0.67 resp. 0.77 if skipping the last one and a half hours (marked with empty triangles), which had stronger convection.

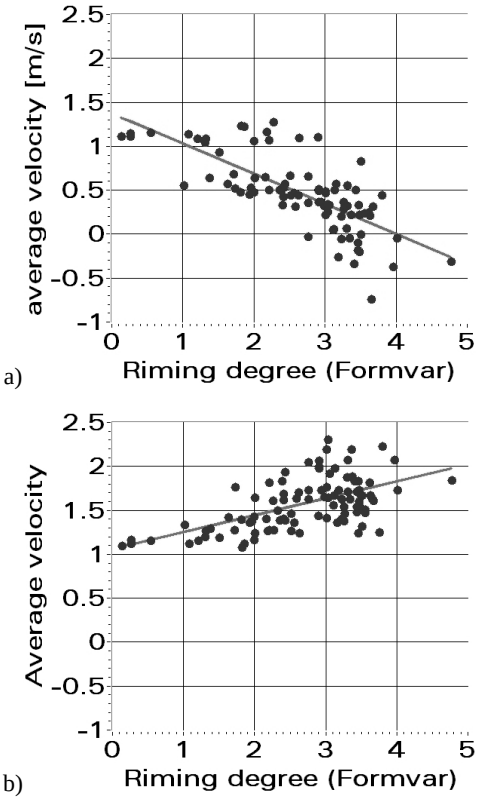

Fig. 6. Averaged Doppler velocity measured by the radar at the height of the top station (a, [m/s]) and Doppler fall velocity measured by the HVSD (b, [m/s]) – both plotted versus degree of riming.

7 Discussion of the case study

The correlation between riming and convectivity, deduced from the straight forward modification of the convection index, is astonishing high. If the regions with a negative Doppler velocity are large – as in the last one and a half hours of our case – an increase of convectivity with higher riming can be seen, which is stronger than the slope of the linear fit. This can possibly be explained by the non-linearity of the riming scale. The increase in rimed mass per riming degree is much smaller for low than for high riming degrees.

Besides, the modified convection index is quite strongly influenced by updrafts. Here, the averaging time for the computation of convection index is equivalent to the relevant time scale of the updrafts and could discriminate between different sizes of embedded convective cells. The different behavior for varying averaging times will be looked at in the future. As a first step (see Sect. 8) the influence of the particle fall speed has been eliminated, to directly get the vertical winds and to separate the influence of steady vertical winds by the in Sect. 5 above described method.

Steady (orographic?) vertical winds are not captured by the convection index. They are likely to have - compared to embedded convective cells - different influence on the relative particle velocities, condensation and the residence time of particles in the clouds. Equation 7 (Klett and Pruppacher, 1997),

$$\frac{dm_1}{dt} \propto \int E_c\,(a_1 + a_2)^2\,(\mathrm{v}_{T,1} - \mathrm{v}_{T,2})\,a_2^3\,n(a_2)\,da_2\,, \qquad (7)$$

is describing the increase in mass of a raindrop (mass m_1, radius a_1) by collecting smaller raindrops ($n(a_2)$ is the quantity for a given radius a_2) with a collection kernel E_c and relative velocities ($\mathrm{v}_{T,1} - \mathrm{v}_{T,2}$). Applying this standard collection equation to riming, it can give us some ideas, what is happening during riming, taking the large collecting raindrop for the ice crystal and the collected smaller raindrops for the supercooled cloud droplets. Besides convectivity and vertical winds, there might be other influencing factors, e.g., concentration, size and habit of ice crystals, and size distribution of cloud droplets, and wind speed and turbulence, influencing the relative velocities.

8 Extension to other cases

Figure 5a shows a scatter plot of convectivity versus riming for all the cases of RAMS I in winter 02/03. For the determination of the degree of riming, Formvar slides have been selected after the following filter rules: the temperature at

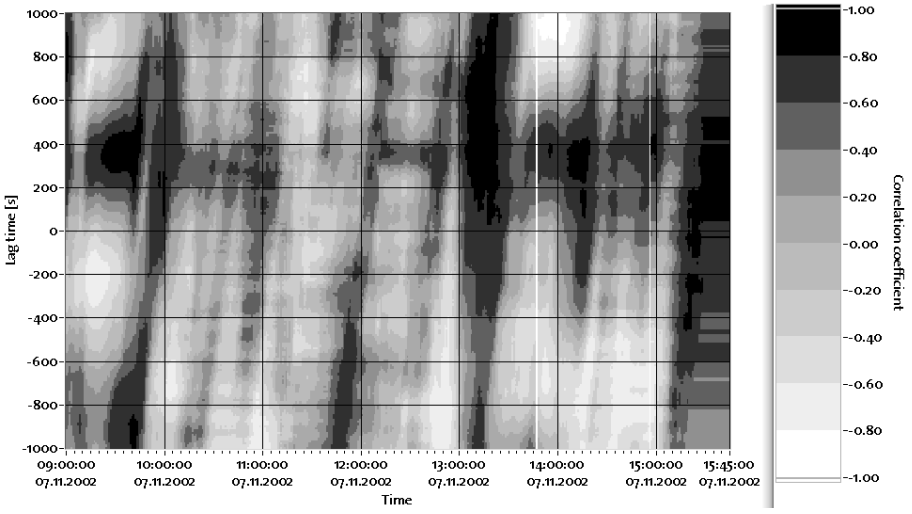

Fig. 7. Lag time field for the case November 7, 2002. The black and white scale gives the correlation coefficients for different lag times (y-scale) at specific times during the case (x-axis).

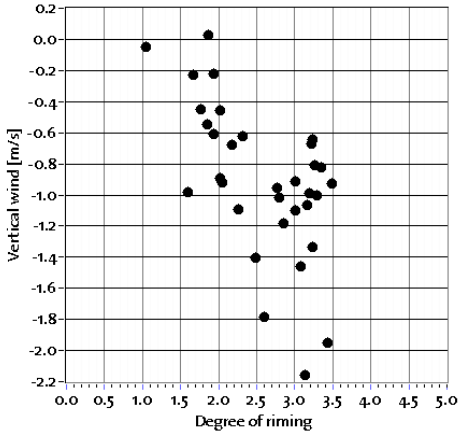

Fig. 8. Scatter plot of with lag time fields re-calculated vertical winds versus degree of riming for the case November 7, 2002.

the top station had to be below $< -1°C$, the rain rate at the bottom station above 0.1 mm/h and furthermore, the lag time had to be below 700 s to make sure, that both measurements where in the same cloud without big developments. The remaining 90 Formvar samples correspond to 900 min of measurements. Again, an increase of convectivity with higher riming can be seen, which is stronger than the one of the linear fit in the above case study. Figure 5b shows for these Formvar samples the corresponding scatter plot of the vertical winds. They have been estimated following the method described in Sect. 5 and are averaged over eleven values, which each have been computed for one minute. The plot is quite similar to the one with the convectivity, but the convection index has the advantage, that only one instrument namely a radar is needed. The above defined convectivity is mainly determined by the vertical winds. This is also depending on the average time, which in future will be investigated in more detail.

Figure 6a shows the average velocity measured by the radar versus riming degree at the height of the mountain station and 6b the Doppler fall velocity measured by the HVSD. The difference between these two plots corresponds to the vertical winds (Fig. 5b). The terminal fall velocity increases as expected with increasing riming. Interestingly, the Doppler velocity measured by the radar is decreasing with increasing riming. For riming of about 3.0 to 3.5 the particles are even in average floating at the measuring height.

9 Conclusions and outlook

For a case study, a correlation could be found between the degree of riming and convectivity, caused by embedded convective cells. They can be seen in the reflectivity and Doppler data of the X-band radar – quantified by a convection index. An application to other case studies shows a similar connection, but with a stronger rise of convectivity for higher riming degrees. This might be due to the non-linear character of the riming scale or a too strong weight for negative average velocities in the modified convection index. Further analysis will have to be done carefully, simpler indices will be tested and meteorological conditions and other microphysical aspects have to be considered. Further plans are e.g. to identify with help of the dual Doppler wind fields special synoptic and orographic situations, which are the reason for the generation of embedded convective cells in stratiform winter precipitation and thus creating prerequisites for riming to occur.

With help of a combination of remote sensing and in-situ measurements and a new method, the particle fall velocities can be eliminated from the Doppler radar velocities and the vertical winds can be estimated. This gives a tool, which is more complicated than the convection index because it needs a second instrument, but directly analyzes the influence of

vertical winds on riming. In the results shown in Fig. 5, the correlation is -0.6 (also -0.6 if restricted to case November 7, 2002) with an application of lag times in sections of a couple of hours. An improved method for lag time correction determines for every minute of measurement an individual lag time. Therefore, for every minute cross-correlations between HVSD and radar data for the surrounding half an hour of measurements have been computed. Figure 7 shows the resulting lag time field for the case November 7, 2002 . Choosing the lag time value with maximum correlation and re-calculating the vertical winds for the case of November 7, 2002, a correlation of -0.6 results (Fig. 8) as above for all cases. If applied to the rest of the cases, a improvement by this method is expected in respect to correlation coefficients resp. spread of data points.

For the combined case studies (Sect. 8) with an increase in riming degree, the fall velocity measured by the HVSD did increase, but the velocity measured by the radar decreased. For a degree of riming of about 3.0–3.5 even in average floating particles where found in free air at the measuring height. This might be an indicator for orographic effects. By upgrading the method for the estimation of vertical winds, even hypotheses for mass-diameter-relations might be testable. Or can such relations - despite of the many influencing factors - even be deduced and thus more information about riming be obtained?

References

Barthazy, E., Göke, S., Schefold, R., and Högl, D.: An optical array instrument for shape and fall velocity measurements of hydrometeors, Journal of Atmospheric and Oceanic Technology, 2004 in press.

Houze, R. A.: Stratiform precipitation in regions of convection: A meteorological paradox?, Bulletin of the American Meteorological Society, 78, 2179, 1997.

Houze, R. A. and Medina, S.: Orographic enhancement of precipiation in midlatitudes: Results from map and improve II, in ICAM/MAP, p. 1, Brig, Switzerland, 2003.

Klett, J. D. and Pruppacher, H. R.: Microphysics of clouds and precipitation, Kluwer Academic Publishers, 1997.

Locatelli, J. D. and Hobbs, P. V.: Fall Speeds and Masses of Solid Precipitation Particles, Journal of Geophysical Research, 79, 2185, 1974.

Mosimann, L.: An Improved Method for Determining the Degree of Snow Crystal Riming by Vertical Doppler Radar, Atmospheric Research, 37, 305, 1995.

Mosimann, L., Weingartner, E., and Waldvogel, A.: An Analysis of Accreted Drop Sizes and Mass on Rimed Snow Crystals, Journal of the Atmospheric Sciences, 51, 1548, 1994.

Poulida, O., Schwikowski, M., Baltensperger, U., Staehelin, J., and Gaeggeler, H. W.: Scavenging of atmospheric constituents in mixed phase clouds at the high-alpine site Jungfraujoch - Part II. Influence of riming on the scavenging of particulate and gaseous chemical species, Atmospheric Environment, 32, 3985, 1998.

Schaefer, V.: The preparation of snow crystal replicas, Weatherwise, 9, 132, 1956.

Schefold, R.: Messungen von Schneeflocken: Die Fallgeschwindigkeit und eine Abschätzung weiterer Grössen, ETH. DISS. Nr. 15431, 2004.

Wüest, M.: Dealiasing Wind Information from Doppler Radar for Operational Use, ETH. DISS. Nr. 14378, 2001.